Grazing Incidence Prompt Gamma Emissions and Resonance-Enhanced Neutron Standing Waves in a Thin Film

Huai Zhang,[1,2] P. D. Gallagher,[1] S. K. Satija,[1] R. M. Lindstrom,[3] R. L. Paul,[3] T. P. Russell,[4] P. Lambooy,[4] and E. J. Kramer[5]

[1]*Reactor Radiation Division, National Institute of Science and Technology, Gaithersburg, Maryland 20899*
[2]*Department of Material and Nuclear Engineering, University of Maryland, College Park, Maryland 20742*
[3]*Inorganic Analytical Research Division, National Institute of Science and Technology, Gaithersburg, Maryland 20899*
[4]*IBM Almaden Research Center, 650 Harry Road, San Jose, California 95120*
[5]*Department of Materials Science and Engineering and the Materials Science Center, Cornell University, Ithaca, New York 14853*
(Received 7 February 1994)

We report simultaneous measurements of neutron-capture prompt gamma emissions as well as neutron reflectivity on a polymer film with an embedded Gd layer. Enhanced γ-ray signals and reduced neutron reflectivity were observed when the neutron standing waves were resonantly amplified in the film. Fitting of both the γ-ray and reflectivity data is of significant aid in uniquely characterizing the depth profile of the polymer film as well as locating the Gd layer.

PACS numbers: 61.80.Ed, 07.85.+n, 61.12.Ex

X-ray standing waves (XSW) generated above a mirror surface during total external reflection have been employed in conjunction with x-ray fluorescence (XF) emissions to locate unambiguously a heavy atomic layer embedded in a biological membrane situated above the highly reflective mirror surface [1–3]. Since biological membranes are mainly comprised of low atomic number Z elements, they are essentially transparent to x rays. Hence, the incident and reflected x-ray beams have equal amplitudes and superpose to form standing waves in the membrane. If a crest of the standing waves encounters a high-Z layer as the x-ray incident angle varies, then, due to the photoelectric effect, fluorescence of the high-Z element occurs. This nondestructive technique has provided a molecular yardstick for studying buried layers in biological membranes.

Similar to the x-ray case, neutron standing waves (NSW) can be combined with neutron-capture prompt gamma emissions (PGE) to locate buried layers in thin films and multilayers. This technique is not limited to low-Z materials because most materials are transparent to thermal and cold neutrons. In spite of the conceptual similarity to XSW and XF, however, NSW and PGE have not been reported previously as a joint experimental technique, mainly because of low neutron beam intensities. Recent observations of resonance-enhanced XSW [4,5] and NSW [6,7] in thin films suggest the feasibility of doing such experiments with neutron beams. It is found that when their spatial period matches the film thickness, the amplitude of the standing waves may be many-fold amplified. In particular, if a cap layer of higher scattering potential is placed on top of the film, then together with the reflecting mirror it forms a (pseudo) potential well, causing neutrons to dwell much longer in the film: The standing wave amplitude is amplified. A twentyfold enhancement of the x-ray flux in thin films has been observed experimentally [4,5], while theoretically the enhancement factor is only limited by absorption, structural imperfections, and the wave vector spread $\Delta k/k$ of the incident beam. Consequently, the resonance-enhanced neutron standing waves (RENSW) would cause an enhanced γ-ray signal.

In this Letter, we present a concise theoretical framework of RENSW and PGE along with experimental results on a polymer film with an embedded Gd layer. We fitted both the γ-ray and neutron reflectivity data, which are of significant aid in uniquely characterizing the depth profile of the polymer film as well as locating the Gd layer.

We consider a cap-film-substrate layered system first in an ideal condition where nuclear absorption, incoherent and phonon scattering, and structural imperfections such as interface roughness and modulation are negligible. We approximate each layer by a homogeneous continuum and start with the one-dimensional (1D) Schrödinger equation describing the stationary state of a neutron incident at an angle θ and wavelength λ. Let $k_x = (2\pi/\lambda) \times \sin\theta$ be the normal component of the $\mathbf{k}$ vector. The Schrödinger equation is

$$\frac{d^2\psi(x)}{dx^2} + [k_x^2 - u(x)]\psi(x) = 0 , \tag{1}$$

with

$$u(x) = \begin{cases} 0, & x < 0, \\ u_c, & 0 \le x < d_c , \\ u_f, & d_c \le x < d_c + d_f , \\ u_s, & x \ge d_c + d_f . \end{cases} \tag{2}$$

where u_c, u_f, and u_s are real constants representing the 1D scattering potentials of the cap layer, the film, and the substrate, respectively, and d_c and d_f are the cap-layer thickness and the film thickness, respectively. For each layer the 1D scattering potential u equals $4\pi Nb$ where N

0031-9007/94/72(19)/3044(4)$06.00

is the number density and b the coherent nuclear scattering length of the nuclei [8]. In general, however, the 1D scattering potential $u(x)$ is complex if nuclear absorption is present [9]. We assume that $u_f < k_x^2 < \{u_c, u_s\}$ and denote $\kappa_c = (u_c - k_x^2)^{1/2}$, $k_f = (k_x^2 - u_f)^{1/2}$, and $\kappa_s = (u_s - k_x^2)^{1/2}$. Then $\psi(x)$ can be written as

$$\psi(x) = \begin{cases} \exp(ik_x x) + r\exp(-ik_x x), & x < 0, \\ t_c \exp(-\kappa_c x) + r_c \exp(\kappa_c x), & 0 \le x < d_c, \\ t_f \exp(ik_f x) + r_f \exp(-ik_f x), & d_c \le x < d_c + d_f, \\ t_s \exp(-\kappa_s x), & x \ge d_c + d_f, \end{cases} \tag{3}$$

where t_i and r_i are the transmittance and reflectance at the bottom interface of the layer denoted by the subscript. From Eq. (1), $\psi^*(d\psi/dx) - \psi(d\psi^*/dx)$ is independent of x, so we have

$$\begin{aligned} 2ik_x(1 - |r|^2) &= 2\kappa_c(t_c^* r_c - r_c^* t_c) \\ &= 2ik_f(|t_f|^2 - |r_f|^2) = 0, \end{aligned} \tag{4}$$

and hence $|r| = 1$ and $|t_f| = |r_f|$, which means that in the x direction ψ forms standing waves above the cap layer with $|\psi|^2_{\max} = 4$ and in the film with $|\psi|^2_{\max} = 4|r_f|^2$. Resonance enhancement in the film means $|r_f|^2 > 1$. The analytic solution of $|r_f|^2$ is

$$|r_f|^2 = \frac{4k_x^2\kappa_c^2}{(k_x^2+\kappa_c^2)(\kappa_c^2+k_f^2)} \frac{1}{|\exp(\kappa_c d_c - i\phi_{xc})\sin(k_f d_f + \phi_{fc} + \phi_{fs}) - \exp(-\kappa_c d_c + i\phi_{xc})\sin(k_f d_f - \phi_{fc} + \phi_{fs})|^2}, \tag{5}$$

where

$$\phi_{xc} = \tan^{-1}(k_x/\kappa_c), \quad \phi_{fc} - \tan^{-1}(k_f/\kappa_c),$$

and

$$\phi_{fs} = \tan^{-1}(k_f/\kappa_s).$$

In the large-d_c limit such that $\exp(\kappa_c d_c) \gg 1$, Eq. (5) becomes very large if $\sin(k_f d_f + \phi_{fc} + \phi_{fs})$ is zero, i.e., if

$$k_f d_f + \phi_{fc} + \phi_{fs} = n\pi. \tag{6}$$

The physics behind the resonance condition [Eq. (6)] can be understood as follows. If we ignore ϕ_{fc} and ϕ_{fs} for a moment, then $k_f d_f = n\pi$ means that d_f is a multiple of the spatial period of the standing waves, where n denotes the harmonics or modes. Adding ϕ_{fc} and ϕ_{fs} means that the effective thickness of the resonator is larger than d_f, because the quantum-mechanical wave function ψ can extend into classically forbidden regions, beyond the walls of the potential well. When Eq. (6) is satisfied,

$$\begin{aligned} |r_f|^2 &= \frac{4k_x^2\kappa_c^2}{(k_x^2+\kappa_c^2)(\kappa_c^2+k_f^2)} \frac{\exp(2\kappa_c d_c)}{\sin^2(2\phi_{fc})} \\ &= \frac{1 - u_f/u_c}{1 - u_f/k_x^2} \exp(2\sqrt{u_c - k_x^2}\, d_c), \end{aligned} \tag{7}$$

which is greater than 1. Two observations can be made from Eq. (7). First, the thicker the cap layer, the larger the enhancement factor $|r_f|^2$ [10]. Second, $|r_f|^2$ is larger at a smaller resonance k_x. Both conclusions need to be modified when nuclear absorption is considered.

When a neutron-absorbing layer with a complex scattering potential $u = u_{\mathrm{Re}} - iu_{\mathrm{Im}}$ [9] is embedded in the film, where $u_{\mathrm{Im}} = 2\pi\mu/\lambda$ and μ is the linear absorption coefficient, then from Eq. (1)

$$d[\psi^*(d\psi/dx) - \psi(d\psi^*/dx)]/dx = -2iu_{\mathrm{Im}}|\psi|^2$$

in the absorbing region and 0 elsewhere. Integrating this equation from $x = -\infty$ to $+\infty$ gives $1 - |r|^2 = (1/k_x) \times \int_X |\psi|^2 u_{\mathrm{Im}} dx$, where X indicates the absorbing region. If more than one absorbing elements (or isotopes) are present, then

$$1 - |r|^2 = \frac{1}{k_x} \sum_i \int_{X_i} |\psi|^2 u_{\mathrm{Im}}^i dx = \sum_i \tau_i, \tag{8}$$

where $\tau_i = (1/k_x)\int_{X_i} |\psi|^2 u_{\mathrm{Im}}^i dx$ is the neutron-capture rate (neutrons/sec) of the i element or isotope normalized to the incident beam intensity. Experimentally, the normalized γ-ray intensity is $C\tau_i$ where C is a constant representing the counting efficiency. Since $\tau_i \le 1$ [Eq. (8)], i.e., $\int_{X_i} |\psi|^2 u_{\mathrm{Im}}^i dx \le k_x$, $|\psi|^2$ has an upper bound, even if $d_c \to \infty$, and this upper bound tends to be smaller at a smaller resonant k_x.

The inset of Fig. 1 is a schematic diagram of the sample. Approximately 0.6 μm thick Ni was first evaporated onto a polished Si substrate 5.1 cm in diameter. A film of polyvinylcyclohexane (PVCH) ($\sim$720 Å in thickness) was spin coated onto the Ni. Subsequently, a 50 Å layer of Gd was evaporated onto the PVCH film. No precaution was taken to prevent the oxidation of the Gd to Gd_2O_3. A film of PVCH ($\sim$720 Å) was floated onto the surface of de-ionized water and retrieved using the substrate, thereby entrapping the Gd between two layers of PVCH. After drying, a predeuterated polystyrene (*d*-PS) film was placed on top of the PVCH in an analogous manner.

The neutron experiments were carried out at the NG7 reflectometer at CNRF in NIST [11]. The sample was mounted horizontally and a γ-ray detector was installed above the sample. The active element of the detector was a high-purity Ge crystal 64 mm in diameter, placed $\sim$10 mm from the sample. The absolute efficiency, measured with calibrated radioactive sources, was 0.10 and 0.09 photopeak counts per photon at $E_\gamma = 181.9$ and 199.2 keV, from capture in ^{157}Gd and ^{155}Gd, respectively. The monochromated neutrons had an average wavelength of

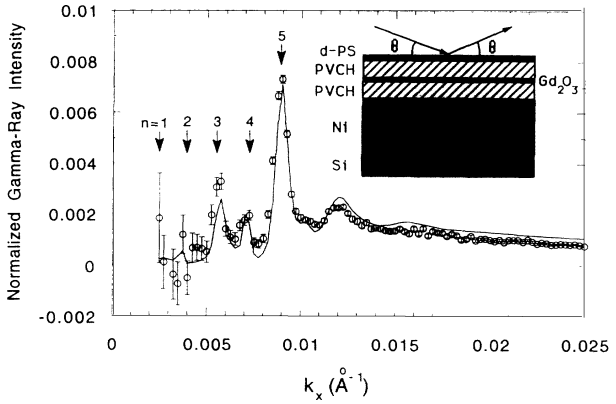

FIG. 1. Gamma-ray data at $E_\gamma = 181.9$ keV from the neutron capture in ^{157}Gd. Circles are measured γ-ray intensity normalized to the incident neutron beam intensity. The arrows indicate the resonance-k_x positions of the RENSW for $n = 1, 2, \ldots,$ and 5 modes. The solid line is the calculated neutron-capture rate multiplied by a constant representing the counting efficiency. Fitting to the data is very sensitive to the location and depth profile of the Gd layer. The inset is a schematic diagram of the sample.

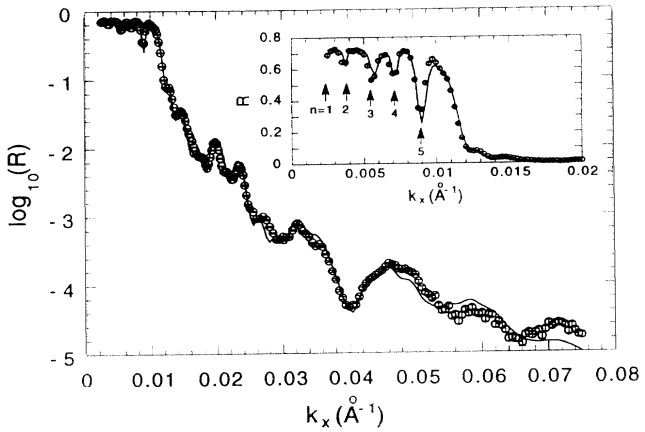

FIG. 2. The measured neutron reflectivity on a log scale. The inset is the low-k_x portion of the data plotted on a linear scale. Solid lines are results of fitting to the data.

$\lambda = 4.1$ Å with $\Delta\lambda/\lambda = 0.025$. The illuminated area of the sample was kept fixed at $\sim 35 \times 40$ mm^2 by continuously opening the beam-defining slits as the incident angle θ increased. Gamma-ray intensities at $E_\gamma = 181.9$ and 199.2 keV were measured from $k_x = 0.00025$ Å^{-1} to 0.075 Å^{-1} with resolution $\Delta k_x/k_x \cong 0.058$. Neutron reflectivity data were taken simultaneously with the γ-ray data at each k_x.

Figure 1 shows the low-k_x portion of the γ-ray data (circles) at $E_\gamma = 181.9$ keV, with the γ counts normalized to the incident beam intensity. Below the critical k_x (0.0107 Å^{-1}) of Ni, five modes of RENSW were expected as indicated by the arrows, and the γ-ray peaks for $n = 3$, 4, and 5 modes were well resolved experimentally. The solid line is the calculated neutron-capture rate τ for ^{157}Gd, multiplied by a constant C, with the sample structural parameters as well as C fit to the data.

A matrix method [12] was used to calculate the neutron wave function $\psi(x)$ and the resulting neutron-capture rate τ, as well as the neutron reflectivity. Interface roughness was modeled by smearing the abrupt change in the 1D scattering potential at each interface with a hyperbolic tangent function, and the roughness was parametrized by the full width at half maximum of the first derivative of the smearing function. The fitting of the calculated γ-ray intensity to the data was sensitive to the total thickness of the PVCH film since the k_x values of the resonance peaks were most affected by the film thickness. The relative intensities of the peaks were very sensitive to the depth and depth profile of the Gd layer. For example, since the Gd layer is located at a trough of the RENSW for the $n = 4$ mode [see Fig. 3(a)], the γ-ray intensity of the $n = 4$ peak depends crucially on how the Gd layer overlaps with the neutron probability density $|\psi(x)|^2$. To obtain a reasonable fit to the data the thickness of the Gd layer was increased to ~ 84 Å with a density only $\sim 86\%$ that of the bulk (which might indicate that the Gd layer was oxidized), and the roughness of both interfaces of the Gd layer was found to be ~ 14 Å. The PVCH film thickness was found to be 737 Å above the Gd layer and 741 Å below it, and the fitting to the data persistently showed a thicker PVCH film at the bottom. The sensitivity of the PGE and RENSW technique to the Gd layer depth and depth profile surpasses that of neutron reflectivity analysis alone. The d-PS film thickness was found to be 240 Å. The real part of the resulting scattering potential $u(x)$ is plotted as the thick solid curve in Fig. 3. The imaginary parts u_{Im} for Gd and PVCH were 3.4×10^{-5} and 9.2×10^{-8} Å^{-2}, respectively.

Figure 2 shows the measured neutron reflectivity on a log scale while the inset shows the low-k_x portion on a linear scale. The solid curves were calculated with the same parameters as used in calculating the solid curve in Fig. 1 for the γ-ray intensity. Since the reflectivity analysis was sensitive to the interface roughness of the d-PS and Ni layers, we also fitted the data to help determine these parameters, and fed them back when we fitted the γ-ray data. The γ-ray and the neutron reflectivity results are in excellent agreement, and indeed they are complementary tools to pin down the depth-profile of the entire sample.

The thin solid lines in Fig. 3 show the neutron probability density $|\psi(x)|^2$ in the $n = 4$ (a) and 5 (b) modes, numerically calculated with the same depth-profile parameters used for the solid lines in Figs. 1 and 2. Tails of $\psi(x)$ extend into the potential walls on both sides, as we expect from the model calculation. For the $n = 4$ mode, even with absorption and structural imperfections included, the standing waves are still resonantly amplified to

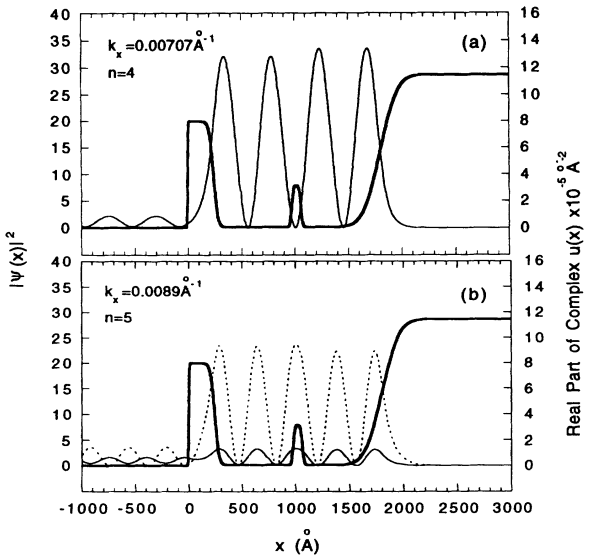

FIG. 3. The real part of the 1D scattering potential $u(x)$ (thick solid lines) obtained from fitting to the γ-ray and neutron reflectivity data, and the neutron probability density $|\psi(x)|^2$ (thin solid lines) calculated accordingly with $k_x = 0.00707$ Å^{-1} (a) and 0.0089 Å^{-1} (b), respectively. For the $n=4$ mode $|\psi|^2_{\max}$ is resonantly amplified to ~ 33 in the PVCH film. The RENSW is suppressed by the absorption in the $n=5$ mode. The dotted line in (b) is $|\psi(x)|^2$ calculated with the imaginary part of $u(x)$ in the Gd layer turned off.

$|\psi|^2_{\max} \sim 33$. For the $n=5$ mode, however, the RENSW is suppressed by the absorption. As a comparison, $|\psi(x)|^2$ is calculated with the imaginary part of $u(x)$ from the Gd layer turned off, plotted as the dotted line in Fig. 3(b). To estimate analytically the suppression effect, we apply the inequality $\int_X |\psi(x)|^2 u_{\mathrm{Im}}(x)dx \leq k_x(n=5)$ to the Gd layer. Since $|\psi(x)|^2 \simeq |\psi|^2_{\max}$ in this region, we get $|\psi|^2_{\max} \leq 0.0089$ Å^{-1}/(3.4×10^{-5} Å^{-2}×84 Å), or $|\psi|^2_{\max} \leq 3.1$, in excellent agreement with the numerical result shown in Fig. 3(b).

In summary, we have demonstrated that PGE combined with RENSW is a sensitive, nondestructive technique for characterizing buried layers of neutron-absorbing nuclei in thin films. The unique properties of neutrons make it particularly applicable to high-Z films such as rare-earth thin films and multilayers where the XF and XSW technique cannot be utilized. Even though in this test of the technique a strong neutron absorber, Gd, is selected for the buried layer, improved sample engineering and more intense neutron beams soon available at the Advanced Neutron Source will allow us to study buried layers of various neutron-absorbing nuclei.

We would like to thank F. S. Bates and M. Gehlsen for providing the PVCH material. We would also like to thank C. F. Majkrzak, Y. P. Feng, and L. J. Norton for discussions on RENSW. Research at Cornell is supported by the NSF, DMR 92-23099.

[1] M. J. Bedzyk, D. H. Bilderback, G. M. Bommarito, M. Caffrey, and J. S. Schildkraut, Science **241**, 1788 (1988); Jin Wang, M. J. Bedzyk, T. L. Penner, and M. Caffrey, Nature (London) **354**, 377 (1991), and references therein.

[2] A. Król, C. J. Sher, and Y. H. Kao, Phys. Rev. B **38**, 8579 (1988).

[3] D. K. G. de Boer, Phys. Rev. B **44**, 498 (1991).

[4] Jin Wang, M. J. Bedzyk, and M. Caffrey, Science **256**, 775 (1992).

[5] Y. P. Feng, S. K. Sinha, H. W. Deckman, J. B. Hastings, and D. P. Siddons, Phys. Rev. Lett. **71**, 537 (1993).

[6] L. J. Norton, E. J. Kramer, R. A. L. Jones, F. S. Bates, H. R. Brown, G. P. Felcher, and R. Kleb, J. Phys. II (France) **4**, 1 (1994).

[7] Y. P. Feng, C. F. Majkrzak, S. K. Sinha, D. G. Wiesler, H. Zhang, and H. W. Deckman, Phys. Rev. B **49**, 10814 (1994).

[8] E. Fermi and W. Zinn, Phys. Rev. **70**, 103 (1946).

[9] L. I. Schiff, *Quantum Mechanics* (McGraw-Hill, New York, 1955), Chap. 5, Sec. 20.

[10] One may intuitively expect a very small amplitude of the standing waves in the film at a very large d_c since a thicker cap layer presents a larger tunneling barrier into the film. However, for a large but finite d_c, it only takes longer for the RENSW to build up. Once the stationary state is reached, the standing waves do not cost energy in the absence of dissipative processes (such as nuclear absorption), and therefore $|\psi|^2_{\max}$ can remain very large in the film. The calculations in Ref. [6], which showed a maximum in $|\psi|^2_{\max}$ vs d_c, were done with a finite u_{Im} in the film.

[11] S. K. Satija and P. D. Gallagher (to be published).

[12] A neutron version of the matrix method used in Ref. [2].

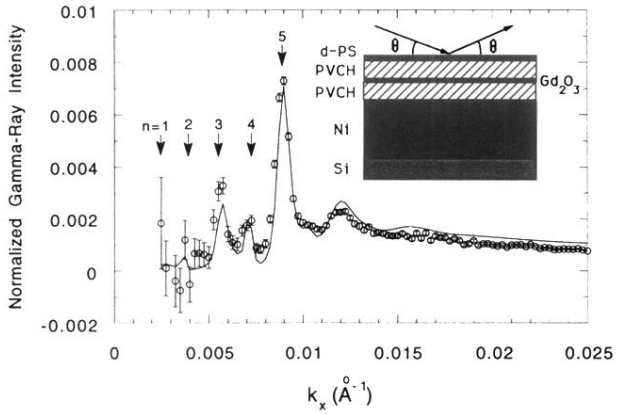

FIG. 1. Gamma-ray data at $E_\gamma = 181.9$ keV from the neutron capture in ^{157}Gd. Circles are measured γ-ray intensity normalized to the incident neutron beam intensity. The arrows indicate the resonance-k_x positions of the RENSW for $n = 1, 2, \ldots,$ and 5 modes. The solid line is the calculated neutron-capture rate multiplied by a constant representing the counting efficiency. Fitting to the data is very sensitive to the location and depth profile of the Gd layer. The inset is a schematic diagram of the sample.